 CMES, vol.30, no.2, pp.57-64, 2008

Analysis of the interaction between two nanovoids using bipolar coordinates

Shuling Hu[1] **and Shengping Shen**[1,2]

Abstract: The effects of surface energy on the interaction between two voids of equal size are investigated. The problem is solved by series expansion in bipolar coordinates. The results show that the surface energy significantly affects the stress concentration around the holes as the size of the holes shrinks to nanometers, meanwhile the interaction between the holes also influences the stress distribution around the holes, which become evident as the holes close to each other. This problem is of great importance in engineering applications.

Keyword: Effect of surface, Voids, Nanometer scale, Bipolar coordinates

1 Introduction

At nanometer scale, the size effects become prominent due to the increasing ratio of surface area to volume. Using molecular dynamic simulations, Zhou and Huang (2004) demonstrated that the effective elastic modulus of a thin free-standing film can either increase or decrease as the film thickness decreases depending upon the crystallographic orientations. Nair *et al*. (2008) investigated the indentation response of Ni thin films of thicknesses in the nano scale using molecular dynamics simulations with embedded atom method interatomic potentials. The observed loading curves are dependent on the film thickness. Solano *et al*. (2008) analyzed the buckling of hexagonal layers in bulk and nanostructures of AlN in the framework of atomistic and first principles techniques, and investigated the size dependence of their structural and electronic properties. Pan *et al*. (2008) presented an analytical method for calculating the Quantum-dot-induced elastic field in anisotropic half-space semiconductor substrates, that is formulated as an Eshelby inclusion problem in continuum mechanics. Classical elasticity does not take into account the effects of surface energy. Dingreville *et al*. (2005) developed a continuum mechanics framework to incorporate the surface free energy and showed that the overall elastic behavior of structural elements (such as particles, wires, films) is size-dependent. Gurtin and Murdoch (1975) and Gurtin *et al*. (1998) developed the theory of surface elasticity, where a surface is regarded as a negligibly thin membrane adhered to the bulk without slipping. As the advent of nanotechnology, the surface elastic theory, developed by Gurtin and his colleagues, has found many applications at nanoscale. For example, Gao *et al*. (2006) developed the finite element formula to take into account the surface effects by using the "surface element". Sharma *et al*. (2003) investigated the deformation around a spherical nanoinhomogeneity, Wang and Wang (2006) studied the effects of surface on the stress field around an elliptical hole, and Yang (2004) derived the effective modulus of elastic materials with nanovoids.

Up to now, most of the researches are limited to a single nanosized void to avoid the interaction effect. However, the interaction between voids is of great importance in engineering application. Ling (1948) and Green (1940) had investigated the interaction problem between two circular holes. However, the surface effect has been neglected in all those investigations and may be important when the holes are in the nanometer range. Most recently, Mogilevskaya *et al*. (2008) investigate the problem of multiple interacting inhomogeneities and/or voids with surface effects based on the complex form of Somigliana's traction identity. But, the solving procedure is very

[1] MOE Key Laboratory for Strength and Vibration, School of Aerospace, Xi'an Jiaotong University, Xi'an 710049, China

[2] Corresponding author. E-mail: sshen@mail.xjtu.edu.cn

complicated. In this paper, we investigate the effects of surface energy on the interaction between two voids of equal size based on Gurtin's theory of surface elasticity, which plays an important role in the mechanical behavior and reliability of porous materials. This problem is best treated by using a bipolar coordinate system, and the solving procedure is much simpler. The detailed introduction of the bipolar coordinate system can be found in Cokker and Filon (1931) and Jeffery (1921).

2 Basic equations in bipolar coordinates

According to the theory of surface elasticity (Gurtin and Murdoch, 1975, 1978; Gurtin, *et al*. 1998), the surface stress tensor $\sigma^s_{\alpha\beta}$ is related to the surface energy density $\Gamma\left(\varepsilon_{\alpha\beta}\right)$ by

$$\sigma^s_{\alpha\beta} = \tau_0\delta_{\alpha\beta} + \frac{\partial\Gamma}{\partial\varepsilon_{\alpha\beta}} \tag{1}$$

where $\varepsilon_{\alpha\beta}$ is the 2×2 surface strain tensor, $\delta_{\alpha\beta}$ the Kronecker delta, and τ_0 the residual surface tenson under unstrained conditions. The partial derivatives are taken at constant surface strain. It is noted that in equation (1) $\varepsilon_{\alpha\beta}$ is not the surface strain tensor but the bulk tensor extrapolated to the surface (Muller and Saul, 2004). Conventional summation rules apply for all repeated Latin indices (1, 2, 3) and Greek subscripts (1, 2) unless otherwise noted.

In the bulk, the equilibrium and isotropic constitutive relations are still expressed as

$$\sigma_{ij,j} = 0 \tag{2}$$

$$\sigma_{ij} = 2\mu\varepsilon_{ij} + \lambda\varepsilon_{kk}\delta_{ij} \tag{3}$$

where σ_{ij} and ε_{ij} are the stress tensor and strain tensor in the bulk materials, respectively. μ and λ are the Lame constants.

By assuming the surface adheres perfectly to the bulk without slipping, according to Gurtin and Murdoch (1975, 1978) and Gurtin *et al*. (1998), the equilibrium equations on the surface can be written as

$$\sigma\mathbf{n} = div_S\mathbf{S} \tag{4}$$

where σ is the stress tensor of the bulk material, $\mathbf{n}$ is the unit vector normal to the surface, $\mathbf{S}$ is the first Piola-Kirchhoff surface stress tensor and div_S represents the surface divergence in its undeformed configuration S. Since the surface tension is small compared to the elastic properties of the material surface, it is neglected in this paper. In this case, the components of the surface stress tensor $\mathbf{S}$ are $\sigma^s_{\alpha\beta}$.Thus, the isotropic constitutive relationships

$$\sigma^s_{\alpha\beta} = 2\mu^s\delta_{\alpha\gamma}\varepsilon_{\gamma\beta} + \lambda^s\varepsilon_{\gamma\gamma}\delta_{\alpha\beta} \tag{5}$$

where μ^s and λ^s are the surface Lame constants for the isotropic surface.

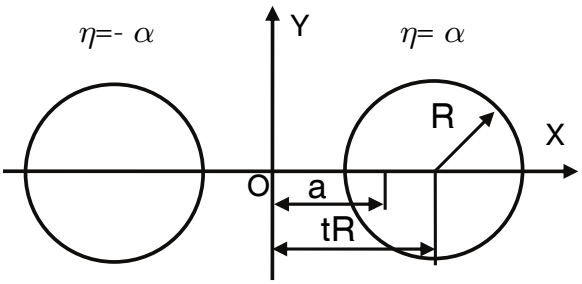

Figure 1: Two holes of equal size.

Now, we consider two circular holes in an infinite isotropic elastic plate under plane strain condition, as shown in Fig. 1. This problem is best treated by using a bipolar coordinate system. A general discussion of stress and strain in bipolar coordinates can be found in Jeffery (1921) and Khomasuridze (2007). The bipolar coordinates (ξ,η) is defined by the following transformation (Jeffery, 1921)

$$x + iy = -a\coth\frac{1}{2}i(\xi + i\eta) \tag{6}$$

such that the two poles of the coordinates are located on the x axis at the points $(\pm a, 0)$, and $x = J\sinh\eta$, $y = J\sin\xi$ with $a/J = \cosh\eta - \cos\xi$. Let the edges of the holes be denoted by $\eta = \pm\alpha$, respectively, and their centers are located symmetrically on the x axis. The radius of the holes $R = a/\sinh\alpha$, and the center is at tR, with $t = \cosh\alpha$ (see Fig. 1).

The biharmonic equation $\nabla^4\chi = 0$ for the stress

function χ then transforms to Jeffery (1921)

$$\left(\frac{\partial^4}{\partial\xi^4}+2\frac{\partial^4}{\partial\xi^2\partial\eta^2}+\frac{\partial^4}{\partial\eta^4}+2\frac{\partial^2}{\partial\xi^2}-2\frac{\partial^2}{\partial\eta^2}+1\right)\frac{\chi}{J}=0 \quad (7)$$

The general solution, even in both ξ and η, can be written as

$$\chi_1/J = K(\cosh\eta-\cos\xi)\ln(\cosh\eta-\cos\xi)+\sum_{n=1}^{\infty}\phi_n(\eta)\cos n\xi \quad (8)$$

with

$$\phi_n(\eta)=A_n\cosh(n+1)\eta+B_n\cosh(n-1)\eta \quad (9)$$

where A_n and B_n are constants to be determined from the boundary conditions. It is required that all the stresses from χ_1 vanish at infinity. When the holes are absent, the stress system in the infinite plate is specified by a symmetrical stress function χ_0. The method of solution when two holes are present is to add χ_1 to χ_0, thus the required stress function can be expressed as

$$\chi=\chi_0+a\sigma_\infty\chi_1 \quad (10)$$

where the factor $a\sigma_\infty$ is introduced to render K, A_n and B_n dimensionless.

The stresses can be derived from χ as:

$$\begin{aligned}\frac{\sigma_{\eta\eta}}{\sigma_\infty}=&\{(\cosh\eta-\cos\xi)\frac{\partial^2}{\partial\xi^2}-\sinh\eta\frac{\partial}{\partial\eta}\\&-\sin\xi\frac{\partial}{\partial\xi}+\cosh\eta\}\frac{\chi}{\sigma_\infty J}\\=&-\frac{1}{2}K(\cosh2\eta-2\cosh\eta\cos\xi+\cos2\xi)\\&+\phi_1(\eta)+\frac{1}{2}\sum_{n=1}^{\infty}\{(n-1)(n-2)\phi_{n-1}(\eta)\\&-2\left(n^2-1\right)\phi_n(\eta)\cosh\eta\\&-(n+1)(n+2)\phi_{n+1}(\eta)\\&-2\phi_n'(\eta)\sinh\eta\}\cos n\xi+\frac{\sigma_{\eta\eta0}}{\sigma_\infty}\end{aligned} \quad (11)$$

$$\begin{aligned}\frac{\sigma_{\xi\xi}}{\sigma_\infty}=&\{(\cosh\eta-\cos\xi)\frac{\partial^2}{\partial\eta^2}-\sinh\eta\frac{\partial}{\partial\eta}\\&-\sin\xi\frac{\partial}{\partial\xi}+\cos\xi\}\frac{\chi}{\sigma_\infty J}\\=&\frac{1}{2}K(\cosh2\eta-2\cosh\eta\cos\xi+\cos2\xi)\\&+\phi_1(\eta)-\frac{1}{2}\phi_1''(\eta)-\frac{1}{2}\sum_{n=1}^{\infty}\{\phi_{n-1}''(\eta)\\&-2\phi_n''(\eta)\cosh\eta+\phi_{n+1}''(\eta)\\&+(n-2)\phi_{n-1}(\eta)-(n+2)\phi_{n+1}(\eta)\\&+2\phi_n'(\eta)\sinh\eta\}\cos n\xi+\frac{\sigma_{\xi\xi0}}{\sigma_\infty}\end{aligned} \quad (12)$$

$$\begin{aligned}\frac{\sigma_{\xi\eta}}{\sigma_\infty}=&-(\cosh\eta-\cos\xi)\frac{\partial^2}{\partial\xi\partial\eta}\left(\frac{\chi}{\sigma_\infty J}\right)\\=&-K\sinh\eta\sin\xi-\frac{1}{2}\sum_{n=1}^{\infty}\{(n-1)\phi_{n-1}'(\eta)\\&-2n\phi_n'(\eta)\cosh\eta\\&+(n+1)\phi_{n+1}'(\eta)\}\sin n\xi\\&+\frac{\sigma_{\xi\eta0}}{\sigma_\infty}\end{aligned} \quad (13)$$

where $\sigma_{\eta\eta0}$, $\sigma_{\xi\xi0}$, $\sigma_{\xi\eta0}$ are derived from χ_0/J, that can be written as

$$\frac{\sigma_{\eta\eta0}}{\sigma_\infty}=\sum_{n=0}^{\infty}c_n\cos n\xi \quad (14)$$

$$\frac{\sigma_{\xi\xi0}}{\sigma_\infty}=\sum_{n=0}^{\infty}e_n\cos n\xi \quad (15)$$

$$\frac{\sigma_{\xi\eta0}}{\sigma_\infty}=\sum_{n=1}^{\infty}b_n\sin n\xi \quad (16)$$

at $\eta=\pm\alpha$. If $\chi_1/J=0$ when $\xi,\eta=0$, all the stresses from χ_1 vanish at infinity, that means

$$\sum_{n=1}^{\infty}(A_n+B_n)=0 \quad (17)$$

For plane strain problems, the strain $\varepsilon_{\xi\xi}$ is obtained as

$$\varepsilon_{\xi\xi}=\frac{1}{2\mu}\left[(1-\nu)\sigma_{\xi\xi}-\nu\sigma_{\eta\eta}\right] \quad (18)$$

where ν is the Poisson's ratio, and the surface stress $\sigma^s_{\xi\xi}$ can be given as

$$\sigma^s_{\xi\xi} = E^s \varepsilon_{\xi\xi} \tag{19}$$

with the surface elastic constants $E^s = 2\mu^s + \lambda^s$. It is noted again, that in this paper we assume the surface tension $\tau_0 = 0$.

The boundary conditions on the circular holes ($\eta = \pm\alpha$) with surface effects are given from Eq. (4) as

$$\begin{aligned} \sigma_{\eta\eta} &= \frac{\sigma^s_{\xi\xi}}{a/\sinh\alpha} \\ \frac{-\sigma_{\xi\eta} n_\eta}{\cosh\alpha - \cos\xi} &= \frac{\partial \sigma^s_{\xi\xi}}{a\partial\xi} \end{aligned} \tag{20}$$

where the normal vector $n_\eta = \mp 1$ for $\eta = \pm\alpha$, respectively. Substituting Eqs. (18) and (19) into the first equation of (20), we can obtain

$$\sigma_{\eta\eta} = D\sigma_{\xi\xi} \tag{21}$$

with

$$D = (1-\nu)\, s/(1+\nu s) \tag{22}$$

and the dimensionless parameter

$$s = E^s/2\mu R \tag{23}$$

s represents the surface effects, the sign of s depends on the sign of the surface elastic constant E^s. If there is no intrinsic surface stress, the surface elastic constant $E^s = 0$, then s=0, the solution reduces to the classical elasticity. When the radius of holes is very large, $s \ll 1$, the surface effects can be neglected and the solution also reduces to that of the classical elasticity at $s = 0$. At the nanoscale, i.e. R falls into $1 \sim 100$nm, s becomes noticeable, and the surface effects are significant.

By combining Eq. (20), we can obtain

$$\frac{-\sigma_{\xi\eta} n_\eta}{\cosh\alpha - \cos\xi} = \frac{\partial \sigma_{\eta\eta}}{\sinh\alpha\partial\xi} \tag{24}$$

Substituting Eqs. (11) and (13) into (24) leads to

$$\begin{aligned} &\psi_{n-1}(\alpha) - 2\cosh\alpha\,\psi_n(\alpha) + \psi_{n+1}(\alpha) \\ &= 6K\delta_{1n} - 6K\cosh\alpha\,\delta_{2n} + 2K\delta_{3n} + 4b_n\sinh\alpha \\ &-2(n-1)c_{n-1} + 4n\cosh\alpha\, c_n - 2(n+1)c_{n+1} \end{aligned} \tag{25}$$

where

$$\begin{aligned} &\psi_n(\alpha) = n(n-1)(n-2)\,\phi_{n-1}(\alpha) \\ &-2n\left(n^2-1\right)\cosh\alpha\,\phi_n(\alpha) + n(n+1)(n+2)\,\phi_{n+1}(\alpha) \end{aligned} \tag{26}$$

Eq. (25) may be replaced by

$$\begin{aligned} \psi_1(\alpha) &= K\left(e^{-3\alpha} - 3e^{-\alpha}\right) - 2c_1 \\ &\quad - 4\sum_{m=1}^{\infty} b_m e^{-m\alpha}\sinh\alpha \end{aligned} \tag{27}$$

and for $n \geq 2$ by

$$\begin{aligned} &\psi_n(\alpha)\sinh\alpha = \\ &\quad [\psi_1(\alpha) + 2c_1]\sinh n\alpha \\ &\quad + 4\sum_{m=1}^{n-1} b_m \sinh(n-m)\alpha\sinh\alpha - 2nc_n\sinh\alpha \\ &\quad - K[\sinh(n-3)\alpha - 3\sinh(n-1)\alpha] + 2K\delta_{2n} \end{aligned} \tag{28}$$

Substituting Eqs. (11) and (12) into (21) leads to

$$\begin{aligned} &\varphi_{n-1}(\alpha) - 2\cosh\alpha\,\varphi_n(\alpha) + \varphi_{n+1}(\alpha) = \\ &De_n - c_n \\ &+ (1+D)K\left(\frac{\delta_{0n}}{2}\cosh 2\alpha - \delta_{1n}\cosh\alpha + \frac{\delta_{2n}}{2}\right) \\ &+ \frac{1-D}{2}\Big[2\phi'_n(\alpha)\sinh\alpha + (n-2)\phi_{n-1}(\alpha) \\ &\quad - (n+2)\phi_{n+1}(\alpha)\Big] \end{aligned} \tag{29}$$

for $n \geq 0$, where

$$\varphi_n(\alpha) = \frac{D}{2}\phi''_n(\alpha) + \frac{1}{2}(n^2-1)\phi_n(\alpha) \tag{30}$$

From Eq. (29), the requirement of the convergence of $\varphi_n(\alpha)$ leads to

$$\begin{aligned} &\frac{(1-D)}{2}\sum_{m=1}^{\infty}\Big[2\phi'_m(\alpha)\sinh\alpha e^{-m\alpha} \\ &+ (m-1)\phi_m e^{-(m+1)\alpha} - (m+1)\phi_m e^{-(m-1)\alpha}\Big] \\ &+ \sum_{m=0}^{\infty}(De_m - c_m)e^{-m\alpha} + (1+D)K\sinh^2\alpha \\ &\qquad = 0 \end{aligned} \tag{31}$$

From Eqs. (17), (27), (28), (29), (31), the coefficients K, A_n and B_n can be determined. Then, the elastic stress field can be obtained.

3 Numerical results and discussion

Three fundamental cases are considered in this paper, namely,

(1) Case 1: the plate is subjected to an all-round tension σ_∞, so that we have

$$\chi_0 = \tfrac{1}{2}\sigma_\infty\left(x^2+y^2\right) \tag{32}$$

or

$$\chi_0/aJ\sigma_\infty = \tfrac{1}{2}\left(\cosh\eta+\cos\xi\right) \tag{33}$$

(2) Case 2: the plate is subjected to a longitudinal tension σ_∞,

$$\chi_0 = \tfrac{1}{2}\sigma_\infty y^2 \tag{34}$$

or

$$\chi_0/aJ\sigma_\infty = \frac{1}{2}\sin^2\xi/(\cosh\eta-\cos\xi) \tag{35}$$

(3) Case 3: the plate is subjected to a transverse tension σ_∞,

$$\chi_0 = \tfrac{1}{2}\sigma_\infty x^2 \tag{36}$$

or

$$\chi_0/aJ\sigma_\infty = \frac{1}{2}\sinh^2\eta/(\cosh\eta-\cos\xi) \tag{37}$$

The stresses at $\eta=\pm\alpha$ derived from function χ_0 are then given by

$$\begin{cases} \frac{\sigma_{\eta\eta}}{\sigma_\infty} & = \frac{\sigma_{\xi\xi}}{\sigma_\infty} = 1 \\ \frac{\sigma_{\xi\eta}}{\sigma_\infty} & = 0 \end{cases} \tag{38}$$

$$\begin{cases} \frac{\sigma_{\eta\eta}}{\sigma_\infty} & = \frac{(1-\cosh\alpha\cos\xi)^2}{(\cosh\alpha-\cos\xi)^2} \\ \frac{\sigma_{\xi\xi}}{\sigma_\infty} & = \frac{\sinh^2\alpha\sin^2\xi}{(\cosh\alpha-\cos\xi)^2} \\ \frac{\sigma_{\xi\eta}}{\sigma_\infty} & = -\frac{\sinh\alpha\sin\xi(1-\cosh\alpha\cos\xi)}{(\cosh\alpha-\cos\xi)^2} \end{cases} \tag{39}$$

and

$$\begin{cases} \frac{\sigma_{\eta\eta}}{\sigma_\infty} & = \frac{\sinh^2\alpha\sin^2\xi}{(\cosh\alpha-\cos\xi)^2} \\ \frac{\sigma_{\xi\xi}}{\sigma_\infty} & = \frac{(1-\cosh\alpha\cos\xi)^2}{(\cosh\alpha-\cos\xi)^2} \\ \frac{\sigma_{\xi\eta}}{\sigma_\infty} & = \frac{\sinh\alpha\sin\xi(1-\cosh\alpha\cos\xi)}{(\cosh\alpha-\cos\xi)^2} \end{cases} \tag{40}$$

for the three cases, respectively.

Thus, for Case 1, we have

$$\begin{aligned} &c_0 = e_0 = 1 \\ &c_n = e_n = b_n = 0 \quad (\forall n \geq 1) \end{aligned} \tag{41}$$

For the other two cases, by expanding the expressions (39) and (40) into Fourier series between $\xi=-\pi$ and $\xi=\pi$ as in Ling (1948), we can obtain

$$\begin{aligned} c_0 &= e^{-\alpha}\cosh\alpha \\ e_0 &= e^{-\alpha}\sinh\alpha \\ c_n &= -e_n = b_n \\ &= 2e^{-n\alpha}\sinh\alpha\left(n\sinh\alpha-\cosh\alpha\right) \quad (\forall n\geq 1) \end{aligned} \tag{42}$$

for Case 2, and

$$\begin{aligned} c_0 &= e^{-\alpha}\sinh\alpha \\ e_0 &= e^{-\alpha}\cosh\alpha \\ c_n &= -e_n = b_n \\ &= -2e^{-n\alpha}\sinh\alpha\left(n\sinh\alpha-\cosh\alpha\right) \quad (\forall n\geq 1) \end{aligned} \tag{43}$$

for Case 3.

It is very interesting to examine the hoop stress along the holes, and define the stress concentration factor (SCF) as

$$\mathrm{SCF} = \left.\frac{\sigma_{\xi\xi}}{\sigma_\infty}\right|_{\eta=\pm\alpha} \tag{44}$$

When the surface effects are included, the SCF depends on the Poisson's ratio ν and the surface elasticity parameter s. In our numerical examples, we keep $\nu=0.26$, just to illustrate the effects of the surface. Due to the symmetry, we only consider the hole at $\eta=\alpha$, and $0\leq\xi\leq\pi$. The dependences of the maximum SCF on t are shown in Figures 2, 3 and 4 for three cases, respectively. In each case, we take s=0., 0.1, and 0.5. The dimensioneless parameter t denotes the distance between the two holes (see Fig. 1). In the all-round tension case (Case 1), the maximum stress is at $\xi=\pi$. In the transverse tension case (Case 3), the maximum stress is at $\xi=\pi$ for $t<2$, and at $\xi=0$

(almost the same as that at $\xi = \pi$) for $t \geq 2$. In the longitudinal tension case (Case 2), this point is less than $\pi/2$. It shifts towards $\xi = \pi/2$ as t increases. The limiting case $t \to \infty$ corresponding to a single hole in the plate, *i.e.* the interaction between the holes is zero. When $t = 1$, the two holes become tangential to each other. As s increases, the maximum stress continuously decreases, while the location of the maximum stress does not chang. For the case of $s = 0$, our results are the same as those of the classical case (Ling, 1948).

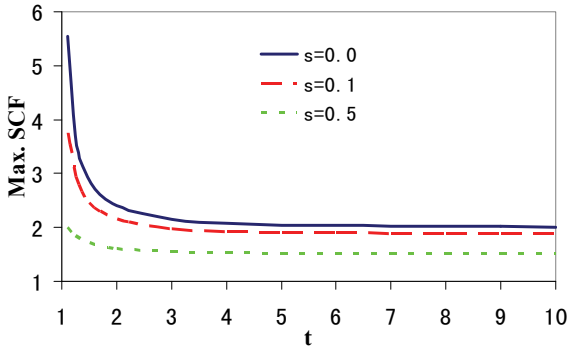

Figure 2: The maximum stress concentration as a function of t in Case 1.

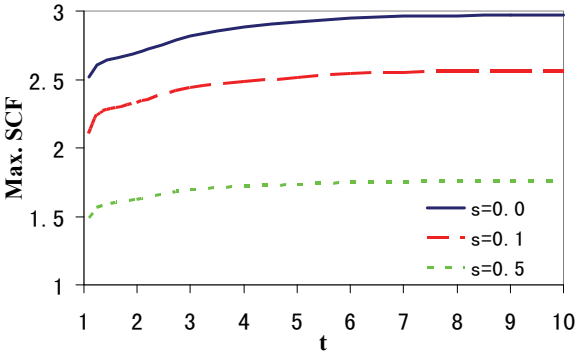

Figure 3: The maximum stress concentration as a function of t in Case 2.

The variation of SCF along the holes under an all round tension (Case 1) for different values of s is plotted in Fig. 5. The variation of SCF along the holes under a longitudinal tension (Case 2) for different values of s (s=0., 0.1, and 0.5) is plotted in Fig. 6. The variation of SCF along the holes

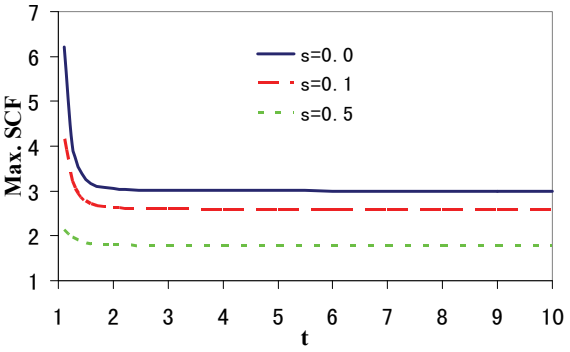

Figure 4: The maximum stress concentration as a function of t in Case 3.

under a transverse tension (Case 3) for different values of s is plotted in Fig. 7. We only present the results at $t = 1.5$. The classical case (without surface effects) corresponds to $s = 0$. In all the three cases, for large value of s, the effect of the surface energy on the SCF around the hole is significant, and the surface energy makes the distribution of stress around the hole even. In Case 1, as s increases, the SCF continuously decreases in the whole range, while it decreases more quickly at $\xi = \pi$ and $\xi = 0$. In Case 2, as s increases, the maximum SCF decreases, while the SCF increases at $\xi = \pi$ and $\xi = 0$ from negative. In Case 3, as s increases, the maximum SCF decreases at $\xi = \pi$ and $\xi = 0$, while the negative SCF increases around $\xi = 0.25\pi$.

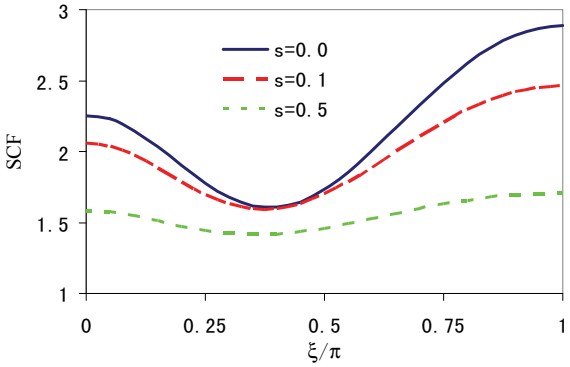

Figure 5: Distribution of SCF around the hole for t=1.5 under an all round tension.

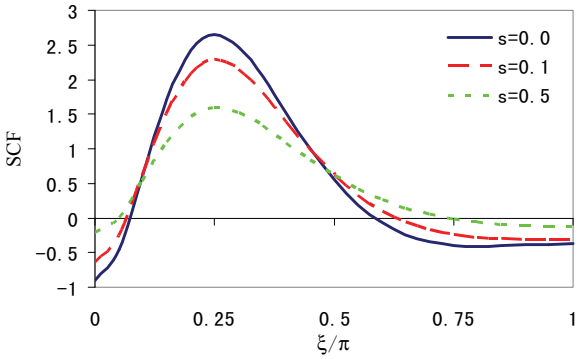

Figure 6: Distribution of SCF around the hole for t=1.5 under a longitudinal tension.

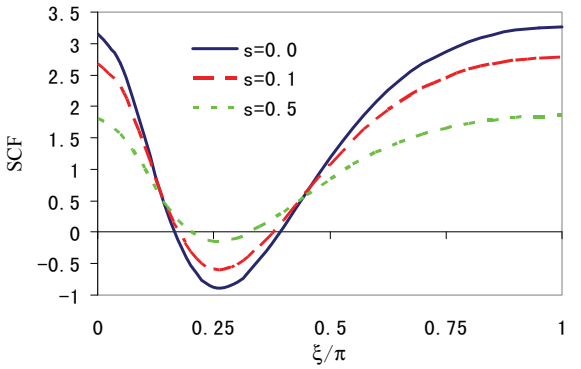

Figure 7: Distribution of SCF around the hole for t=1.5 under a transverse tension.

4 Conclusion

To summarize, we investigated the effects of surface energy on the interaction of two nanosized holes in a plate. Three fundamental stress systems are discussed. Bipolar coordinates are used in the solution. The results indicate that the surface energy significantly affects the stress concentration around the holes when the size of the holes shrinks to nanometers, meanwhile the interaction between the holes also influences the stress distribution around the holes, which become evident as the holes close to each other. For the complicated boundary conditions, numerical methods should be used, especially the multiscale methods, such as Shen and Atluri (2005, 2004), Chung *et al.* (2004), Ma *et al.* (2005), Liu *et al.* (2007), Wallstedt and Guilkey (2007), Chirputkar and Qian (2008), Nishidate *et al.* (2008), and Fitzgerald *et al.* (2008).

Acknowledgement: The supports from NSFC (Grant No. 10672130), Ministry of Education of China (NCET Program), and 973 Program (2007CB707702) are acknowledged.

References

Cokker, E.G.; Filon, L.N.G. (1931): *Photoelasticity*. Cambridge.

Chirputkar, S.U.; Qian, D. (2008): Coupled atomistic/continuum simulation based on extended space-time finite element method. *CMES: Computer Modeling in Engineering & Sciences* 24: 185-202.

Chung, P.W.; Namburu, R.R.; Henz, B.J. (2004): A lattice statics-based tangent-stiffness finite element method. *CMES: Computer Modeling in Engineering & Sciences* 5: 45-62.

Dingreville, R.; Qu, J.; Cherkaoui, M. (2005): Surface free energy and its effect on the elastic behavior of nano-sized particles, wires and films. *Journal of the Mechanics and Physics of Solids* 53: 1827-1854.

Fitzgerald, G.; Goldbeck-Wood, G.; Kung, P.; Petersen, M.; Subramanian, L.; Wescott, J. (2008): Materials modeling from quantum mechanics to the mesoscale. *CMES: Computer Modeling in Engineering & Sciences* 24: 169-183.

Gao, W.; Yu, S.W.; Huang, G.Y. (2006): Finite element characterization of the size-dependent mechanical behaviour in nanosystems. *Nanotechnology* 17: 1118-1122.

Green, A.E. (1940): General biharmonic analysis for a plate containing circular holes. *Proceeding of the Royal Society of Lodon* A 176: 121-131.

Gurtin, M.E.; Murdoch, A.I. (1975): A continuum theory of elastic material surfaces. *Archive for Rational Mechanics and Analysis* 57: 291-323.

Gurtin, M.E.; Murdoch, A.I. (1978): Surface stress in solids. *International Journal of Solids and Structures* 14: 431-440.

Gurtin, M.E.; Weissmuller, J.; Larche, F. (1998): A general theory of curved deformable interfaces in solids at equilibrium. *Philosophical Magazine* A 78: 1093-1109.

Jeffery, G.B. (1921): Plane stress and plane strain in bipolar co-ordinates. *Philosophical Transactiona of the Royal Society of London* A 221: 265-293.

Khomasuridze, N. (2007): Solution of some elasticity boundary value problems in bipolar coordinates. *Acta Mechanica* 189: 207-224.

Ling, C.B. (1948): On the stress in a plate containing two circular holes. *Journal of Applied Physics* 19: 77-82.

Liu, Y.; Zhang, X.; Sze, K.Y.; Wang, M. (2007): Smoothed molecular dynamics for large step time integration. *CMES: Computer Modeling in Engineering & Sciences* 20(3): 177-191.

Ma, J.; Lu, H.; Wang, B.; Roy, S.; Hornung, R.; Wissink, A.; Komanduri, R. (2005): Multiscale simulations using generalized interpolation material point (GIMP) method and SAMRAI parallel processing. *CMES: Computer Modeling in Engineering & Sciences* 8: 135-152.

Mogilevskaya, S.G.; Crouch, S.L.; Stolarski, H.K. (2008): Multiple interacting circular nano-inhomogeneities with surface/interface effects. *Journal of the Mechanics and Physics of Solids*. doi:10.1016/j.jmps.2008.01.001

Muller, P.; Saul, A. (2004): Elastic effects on surface physics. *Surface Science Reports* 54: 157-258.

Nair, A.K.; Farkas, D.; Kriz, R.D. (2008): Molecular dynamics study of size effects and deformation of thin films due to nanoindentation. *CMES: Computer Modeling in Engineering & Sciences* 24: 239-248.

Nishidate, Y.; Nikishkov, G.P. (2008): Atomic-scale modeling of self-positioning nanostructures. *CMES: Computer Modeling in Engineering & Sciences* 26: 91-106.

Pan, E.; Zhang, Y.; Chung, P.W.; Denda, M. (2008): Strain energy on the surface of an anisotropic half-space substrate: Effect of quantum-dot shape and depth. *CMES: Computer Modeling in Engineering & Sciences* 24: 157-167.

Sharma, P.; Ganti, S.; Bhate, N. (2003): Effect of surfaces on the size-dependent elastic state of nano-inhomogeneities. *Appled Physics Letters* 82: 535-537.

Shen, S.; Atluri, S.N. (2004): Multiscale simulation based on the meshless local Petrov-Galerkin (MLPG) method. *CMES: Computer Modeling in Engineering & Sciences* 5: 235-255.

Shen, S.; Atluri, S.N. (2005): A tangent stiffness MLPG method for atom/continuum multiscale simulation. *CMES: Computer Modeling in Engineering & Sciences* 7: 49-67.

Solano, C.J.F.; Costales, A.; Francisco, E.; Pendas, A.M.; Blanco, M.A.; Lau, K.C.; He, H.; Pandey, R. (2008): Buckling in wurtzite-like AlN nanostructures and crystals: Why nano can be different. *CMES: Computer Modeling in Engineering & Sciences* 24: 143-156.

Wallstedt, P.C.; Guilkey, J.E. (2007): Improved velocity projection for the material point method. *CMES: Computer Modeling in Engineering & Sciences* 19(3): 223-232.

Wang, G.F.; Wang, T. J. (2006): Deformation around a nanosized elliptical hole with surface effect. *Appled Physics Letters* 89: 161901.

Yang, F. (2004): Size dependent effective modulus of elastic composite materials: spherical nanocavities at dilute concentrations. *Journal of Applied Physics* 95: 3516-3520.

Zhou, L.G.; Huang, H. (2004): Are surfaces elastically softer or stiffer? *Appled Physics Letters* 84: 1940-1942.